Adaptive Method for the Experimental Detection of Instabilities

Jason S. Anderson, Stanislav Y. Shvartsman, Georg Flätgen, and Ioannis G. Kevrekidis*
Department of Chemical Engineering, Princeton University, Princeton, New Jersey, 08544

Ramiro Rico-Martínez
Departamento de Ingeniería Química, Instituto Tecnológico de Celaya, Celaya, Guanajuato, 38010 México

Katharina Krischer
Fritz-Haber-Institut der Max-Planck-Gesellschaft, Faradayweg 4-6, 14195 Berlin, Germany
(Received 3 August 1998)

Motivated by numerical bifurcation detection, we present a methodology for the direct location of bifurcation points in nonlinear dynamic laboratory experiments. The procedure involves active, adaptive use of the bifurcation parameter(s) as control variable(s), coupled with the on-line identification of low-order *nonlinear* dynamic models from experimental time-series data. Application of the procedure to such "hard" transitions as saddle-node and subcritical Hopf bifurcations is demonstrated through simulated experiments of lumped as well as spatially distributed systems. [S0031-9007(98)08206-4]

PACS numbers: 05.45.Tp, 82.40.Bj

The typical laboratory procedure for obtaining a bifurcation diagram of an experimental system with respect to an operating parameter (the *bifurcation parameter*) involves *setting* the parameter to a fixed value and passively *observing* the dynamics as they asymptotically approach stationary behavior (steady state, stable oscillations, etc.). The operating parameter is then set to a new (fixed) value, and the system is once again allowed to settle. When a qualitative change in the long-term behavior of the system is observed between two consecutive parameter settings, indicating a bifurcation, the *critical* intermediate parameter value is approached through, e.g., interval halving.

This passive "set (parameter) and observe (dynamics)" approach is ubiquitous and straightforward but has obvious shortcomings: trying to locate points of marginal stability (zero, or zero real part eigenvalues) means long experimental transients and inconveniently large settling times. Furthermore, in the detection of "hard" bifurcations as the saddle-node or the subcritical Hopf bifurcation, overstepping the critical parameter value from the "stable side" to the "unstable side" results in the loss (locally) of all stable solutions, and the system will tend to move far away from the neighborhood of phase space which formerly contained the stable steady state. Hysteresis will then complicate the subsequent refining of the experimental bifurcation point estimate.

These problems, which make *accurate experimental bifurcation location* nontrivial, will also be encountered by the modeler who has available only a "direct simulation" algorithm: an integrator where one again *sets* parameter values (and initial conditions) and *observes* (integrates) the dynamics until they settle to stationary behavior.

On the other hand, a modeler can construct different algorithms (numerical bifurcation algorithms [1]); these exploit a model of the system by constructing a strategy for *actively and simultaneously searching phase and parameter space* to locate bifurcation points of the model. The key here is to construct an *inflated* dynamical system (whose state variables are the original state variables plus the operating parameters); this *inflated* system has stable steady states where the original model has marginally stable (bifurcation) points.

It is, of course, impossible to implement "numerical bifurcation algorithms" directly on an experiment. To begin with, an accurate model of the experiment is not available (if it were, the bifurcation points would be located computationally). More importantly, the computational convergence to bifurcation points involves, at each iteration of, say, a Newton-Raphson algorithm, new settings of the state variables and the operating parameter, as determined by the previous step; and while, in an experimental context, we can certainly change the operating parameter "at will," we cannot arbitrarily set the *state* of the system at any given moment; the state is governed by the (experimental) system dynamics.

We attempt to bridge the gap between the passive "set and observe" approach and the experimentally unimplementable "numerical bifurcation approach." This is done by actively using what can be arbitrarily modulated experimentally (the operating parameter) to address what cannot be arbitrarily modulated experimentally (the state variables). Thus we can stabilize a steady state "with an extra condition": criticality in our case ([2,3]; see [4] for an extremum condition).

The procedure involves local, low-order nonlinear models, identified on-line using input/output (I/O) data from the system. On-line identification of local models—linear or nonlinear—plays an important role in detecting and stabilizing unstable states both in theory (e.g., [5,6]) and experiments (e.g., [7,8]), in combination with

 0031-9007/99/82(3)/532(4)$15.00

continuation techniques (e.g., [9,10]). These adaptive, local, approximate nonlinear models are used on-line to (a) estimate the critical parameter value and the critical value(s) of the state variable(s) and to (b) design an *active* parameter variation policy (a "controller") that will bring (quickly) the current state(s) to the critical state(s) and keep it there.

A schematic of the proposed strategy appears in Fig. 1; in this paper the procedure is implemented in discrete time. At the end of each measurement interval, measurements from the experiment (the "unknown system") are (adaptively) used to identify a local nonlinear dynamic model; this incorporates the dependence of the dynamics on the bifurcation parameter (which will be used as the control variable in the closed loop). On-line estimates of the critical parameter value and the value(s) of the state variable(s) at criticality are made based on the adaptive model, using the steady state equations as well as a *test function* [1] quantifying the state's "proximity to bifurcation" (criticality). The critical state and parameter value are (adaptively) estimated by solving (at each time step) this aggregate set of nonlinear algebraic equations using, for example, a Newton-Raphson contraction mapping. The estimated critical state(s) becomes the set point for our controller; at each step we use the (adaptive) model as a reference to determine an appropriate control policy (adjustments in the control variable, which used to be our open-loop bifurcation parameter) that will bring the system *state* to the critical value(s). Subsequent input/output data from the system are used to refine the model and improve estimates of the critical conditions.

For a well-understood experiment the identification may be based on first principles models; we desire a general purpose structure, applicable to systems that are not well understood. For the types of bifurcations we intend to seek, center manifold and normal form theory (e.g., [11]) suggest that in the neighborhood of the bifurcation (in phase $\times$ parameter space) the local long-term dynamics of a system are completely described by low-order polynomials. The appropriateness of such a representation, based on exploiting the separation of time scales due to the existence of a near-critical eigenvalue, motivates our dynamic model structure. We assume that we can instantaneously measure all state variables x_i of the experimental system $x_i(t + \Delta t) = F_i(x(t); p(t))$ viewed in discrete time steps; we identify a model

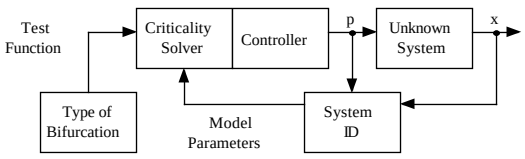

FIG. 1. Schematic of the proposed strategy. I/O data are used to identify a local nonlinear model, which serves as a control reference for driving the system to marginal stability.

of the type $\hat{x}_i(t + \Delta t) \equiv \hat{F}_i(x(t); p(t)) = a_i + \sum_{j=1}^{n} b_{i,j}x_j(t) + c_i p(t) + \sum_{j=1}^{n}\sum_{k=j}^{n} d_{i,j,k}x_j(t)x_k(t) + \sum_{j=1}^{n} e_{i,j}x_j(t)p(t) + f_i p^2(t)$, where p is the bifurcation parameter, n is the dimension of the state space, and a, b, c, d, e, and f are all model parameters (in the detection of Hopf bifurcations we also add cubic terms). The model parameters are obtained by least-squares regression [12] on data sampled at regular intervals (Δt) and are updated after every step. The assumption of measuring *all* state variables can be relaxed.

The steady state equations of this discrete-time model may be expressed as $\hat{F}(x; p) - x = 0$. The criticality constraint used to augment the steady state equations depends on the type of bifurcation being investigated (and the dimensionality of the model); the constraint corresponding to a saddle-node bifurcation point can be posed as $\mathrm{Det}[\nabla_x \hat{F}(x; p) - I] = 0$, where I is an n-dimensional identity matrix and $\nabla_x \hat{F}$ is the Jacobian of the identified model map. For a (nondegenerate, two-dimensional) Hopf bifurcation we use $\mathrm{Det}[\nabla_x F(x; p)] - 1 = 0$. Note that these constraints are for maps, corresponding to the nature of our discrete time model. Estimates $S_{\mathrm{cr}} \equiv (\hat{x}_{\mathrm{cr}}; \hat{p}_{\mathrm{cr}})$ of the experimental critical conditions are obtained by solving (via Newton-Raphson) the model steady state and criticality constraint equations on-line.

We have chosen a couple of simple control laws to determine our control (parameter variation) policy. The first involves the determination, at every step, of the n-element control schedule $[p(t), p(t + \Delta t), \ldots, p(t + (n - 1)\Delta t)]$, which will bring the mpdel from the current state $x(t)$ to the estimated critical state $\hat{x}_{\mathrm{cr}}$ in the smallest number of steps possible. For a one-dimensional system (model) we solve $\hat{F}(x(t); p(t)) - \hat{x}_{\mathrm{cr}} = 0$, but for the two-dimensional case, we need a two-step policy, and we must solve $\hat{F}[\hat{F}(x(t); p(t)); p(t + \Delta t)] - \hat{x}_{\mathrm{cr}} = 0$ for $p(t)$ and $p(t + \Delta t)$. Only the first action $p(t)$ of each solution is implemented experimentally; the parameter is set and held constant over the sampling interval, and the model identification, criticality estimation, and control policy computation steps are repeated until the system converges to its open-loop critical state.

A second, less drastic, control policy, involves control actions that will reduce, in the next time interval, the current distance from criticality by a prescribed amount. In this case we solve for $p(t)$ such that $\|\hat{F}(x(t); p(t)) - \hat{x}_{\mathrm{cr}}\| = C_{\mathrm{frac}}\|x(t) - \hat{x}_{\mathrm{cr}}\|$, where C_{frac} is the targeted fraction of the current distance from (estimated) criticality (say 0.1 or 0.05) and $\|\cdot\|$ denotes the Euclidean norm.

We demonstrate, through a number of simulated experiments, the ability of the method to drive "unknown" systems to open-loop marginal stability, given a suitable initial condition. The first system we consider is a one-dimensional dynamical model of an electrochemical reaction system [13]. The ordinary differential equation models the time dependence of the voltage drop x_1 across an electrical double layer formed at the surface of an

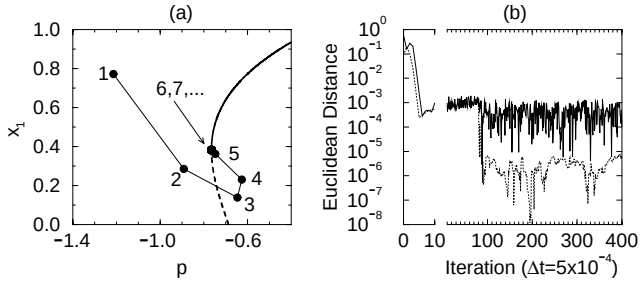

FIG. 2. Convergence to a saddle node in the electrochemical system model. Closed loop transients are overlayed on the open-loop bifurcation diagram in (a); solid (broken) lines indicate stable (unstable) open loop solutions. In (b) the Euclidean distances of the current state $S(t)$ (solid line) and the estimated critical state $\hat{S}_{\rm cr}(t)$ (dashed line) from the actual critical state $S_{\rm cr}$ are plotted as a function of time.

electrode under an applied voltage p:

$$\dot{x}_1 = k_1 + k_2 p + k_3 x_1 + k_4 x_1^3 ,$$

where $k_1 = 1372.55$, $k_2 = 2000.00$, $k_3 = 614.379$, and $k_4 = -1405.23$ are system constants. The system exhibits a saddle-node bifurcation at $S_{\rm cr} \approx (0.381\,754; -0.764\,455)$.

Observing x_1 at discrete time intervals of $\Delta t = 0.0005$, we identified a first local polynomial model after a brief initialization period: for a number of steps, the bifurcation (control) parameter was randomly perturbed around an initial value as the system evolved. Once the initial model was identified, the control algorithm was activated and the steps were conducted as previously described. In order to maintain persistent excitation (thus avoiding numerical difficulties with the identification) a small random perturbation was added to each control action (parameter adjustment); this excitation signal had a maximum amplitude of 5×10^{-4}.

Figure 2a shows the trajectory (sampled at Δt intervals) through the augmented phase space (vertical axis: state variable; horizontal axis: control variable, which used to be the open-loop bifurcation parameter) superposed on the open-loop bifurcation diagram of the system; Fig. 2b shows the time variation of the Euclidean distances of the state $S(t) \equiv (x(t); p(t))$ and estimated critical state $\hat{S}_{\rm cr}(t)$ from the actual critical state $S_{\rm cr}$, respectively. The trajectory is plotted from the time at which the control is activated. The controller rapidly brings the system close to the bifurcation point, and as the model becomes better tuned, the estimate of the critical state gradually improves. Because of the presence of the excitation signal, the system reaches a physical convergence limit at which the state x_1 remains a distance on the order of 10^{-4} away from the critical state. The excitation signal is necessary to avoid undesirable "bursting" due to the deterioration of the identification scheme (a notorious feature of adaptive control schemes [12,14]).

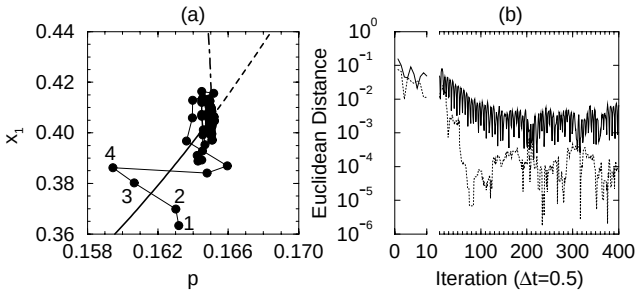

FIG. 3. Convergence to a subcritical Hopf bifurcation point in a stirred tank reactor, analogous to Figs. 2a and 2b. The dot-dashed line in (a) indicates the maximum x_1 values on the open-loop unstable (subcritical) limit cycle.

The second example features the detection of a subcritical Hopf bifurcation in a stirred tank reactor (STR) model [15]:

$$\dot{x}_1 = -x_1 + p(1 - x_1)e^{x_2},$$
$$\dot{x}_2 = -x_2 + pk_1(1 - x_1)e^{x_2} - k_2(x_2 - k_3),$$

where x_1 and x_2 correspond to concentration and temperature, and $k_1 = 14.0$, $k_2 = 3.0$, and $k_3 = 0.0$ are fixed parameters. The Hopf bifurcation with respect to the Damkoehler number p is located at $S_{\rm cr} \approx (0.405\,955, 1.420\,84; 0.165\,042)$. Using a time step of $\Delta t = 0.5$ and an excitation signal amplitude of 1×10^{-4}, we obtained the results shown in Fig. 3. For this example, we have made use of the second control law described, acting to bring the system, at the next step, to 5% of its current distance from estimated criticality. The trajectory of the "experiment" and the bifurcation diagram are both projected into the x_1-p plane in Fig. 3a, clearly showing convergence to the bifurcation point.

Our experimental bifurcation detection strategy can also be applied to dissipative spatially distributed systems in which a separation of time scales results in low-order long-term dynamical behavior. In such cases, most of the eigenvalues in the spectrum lie well away from the

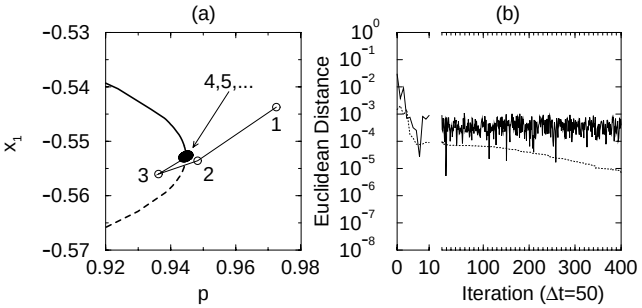

FIG. 4. Convergence to a saddle node in the reaction-diffusion system, analogous to Figs.2a and 2b; the 0th spatial Fourier mode of u is used as the low-dimensional model state x_1.

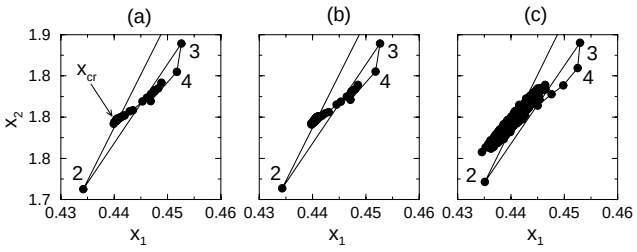

FIG. 5. Effect of noise on the STR Hopf bifurcation detection; closed loop trajectories with (a) 1×10^{-4}, (b) 1×10^{-3}, and (c) 1×10^{-2} maximum amplitude random noise in the control parameter value are shown. The location of the critical state is marked by the arrow in (a).

imaginary axis and only a few have small real parts. Low-dimensional polynomial models are therefore again appropriate for describing the dynamics on a center manifold (or an approximate inertial manifold).

We demonstrate this through a "simulated experiment" of a one-space-dimension, two-variable reaction-diffusion system [16]:

$$u_t = u_{xx} + u - u^3 - v\,,$$

$$v_t = k_1 v_{xx} + p(u - k_2 v - k_3)\,,$$

where u and v are, respectively, activator and inhibitor concentrations, $u_x(0) = u_x(L) = v_x(0) = v_x(L) = 0, L = 20$ and the fixed parameters are $k_1 = 4.0$, $k_2 = 2.0$, and $k_3 = -0.03$. At $p_{\rm cr} \approx 0.944\,654$ a saddle-node bifurcation results in the formation of stable and unstable stationary frontlike solutions of u and v, in addition to the three homogeneous solutions already present. Since the bifurcation to be located is a saddle node, we identified a one-variable dynamic model choosing the spatial average, the 0th Fourier mode ($x_1 \equiv \langle u \rangle$) of the activator concentration, as our state variable; other system "measurements" would have also been successful. We converge on this bifurcation point using a time step $\Delta t = 50$ and a maximum excitation amplitude of 1×10^{-3} (see Fig. 4).

The final set of simulations demonstrates the effect of measurement noise on the strategy. Various levels of noise were added during the detection of the Hopf bifurcation in the STR model (for parameters $k_1 = 7.06$, $k_2 = 0.74$, and $k_3 = 0$, and a time step $\Delta t = 1$). The results are provided in Fig. 5; phase-plane plots of the trajectories in Figs. 5a– 5c correspond to maximum noise amplitudes of 1×10^{-4}, 1×10^{-3}, and 1×10^{-2}, respectively. As expected, for low noise levels the system is able to closely approach the critical state $S_{\rm cr} \approx (0.440\,493, 1.787\,29; 0.131\,802)$, indicated by the arrow in Fig. 5a; with greater noise, the system has more difficulty but manages to remain in the vicinity.

We have demonstrated the successful use of adaptive control techniques for the quick and accurate experimental detection of hard bifurcations, which are problematic for traditional experimental procedures. The general bifurcation detection strategy we have outlined is flexible enough to accommodate numerous types of models, model identification, and control algorithms (e.g., time-delay/embedding based models, projection algorithms, receding horizon control procedures). The extension of the strategy to detect higher codimension bifurcations is also straightforward; it requires modeling the dependence of the system dynamics with respect to a second operating parameter and the consideration of a second criticality constraint. We believe that the algorithms outlined here can greatly facilitate software-assisted experimentation for instability detection. The same algorithms can be used to build a shell around a complex simulation code (a "time stepper") to turn it into a numerical bifurcation code.

We gratefully acknowledge the partial support of NSF, NATO, UTRC, the Humboldt Foundation (R. R., I. G. K.) and the DFG (G. F.).

*Corresponding author.

[1] E. Doedel, H. B. Keller, and J. P. Kernévez, Int. J. Bifurcation Chaos **1**, 493 (1991).
[2] D. G. O'Neil, G. Lyberatos, and S. A. Svoronos, in Proceedings of the AIChE Annual Meeting, Paper 172j, Washington, DC, 1988 (unpublished).
[3] J. S. Anderson, I. G. Kevrekidis, R. Rico-Martínez, and K. Krischer, in *Proceedings of the 30th Annual Conference on Information Sciences and Systems* (Princeton University, Princeton, NJ, 1996), Vol. 1, p. 155.
[4] M. Krstic and H. H. Wang, Automatica (to be published).
[5] E. Ott, C. Grebogi, and J. A. Yorke, Phys. Rev. Lett. **64**, 1196 (1990).
[6] T. Shinbrot, Adv. Phys. **44**, 73 (1995).
[7] V. Petrov, S. Metens, P. Borckmans, G. Dewel, and K. Showalter, Phys. Rev. Lett. **75**, 2895 (1995).
[8] V. Petrov *et al.*, Phys. Rev. Lett. **75**, 3779 (1996).
[9] T. L. Carroll, I. Triandaf, I. Schwartz, and L. Pecora, Phys. Rev. A **46**, 6189 (1992).
[10] I. B. Schwartz, T. W. Carr, and I. Triandaf, Chaos **7**, 664 (1997).
[11] J. Guckenheimer and P. Holmes, *Nonlinear Oscillations, Dynamical Systems, and Bifurcations of Vector Fields* (Springer, Heidelberg, 1983).
[12] G. C. Goodwin and K. S. Sin, *Adaptive Filtering, Prediction, and Control* (Prentice-Hall, Englewood Cliffs, NJ, 1984).
[13] N. Mazouz, K. Krischer, G. Flätgen, and G. Ertl, J. Phys. Chem. B **101**, 2403 (1997).
[14] T. R. Fortescue, L. S. Kershenbaum, and B. E. Ydstie, Automatica **17**, 831 (1981).
[15] A. Uppal, W. H. Ray, and A. B. Poore, Chem. Eng. Sci. **29**, 967 (1974).
[16] A. Hagberg and E. Meron, Nonlinearity **7**, 805 (1994).